Int. J. Morphol.,
41(6):1887-1896, 2023.

Zarzio Ameliorates Non-alcoholic Fatty Liver Induced By a High Fat Diet in a Rat Experimental Model: A Histological and Immunohistochemical Study

Zarzio Mejora el Hígado Graso no Alcohólico Inducido por una Dieta Rica en Grasas en un Modelo Experimental en Ratas: Un Estudio Histológico e Inmunohistoquímico

Tourki A. S. Baokbah

BAOKBAH, T. A. S. Zarzio ameliorates non-alcoholic fatty liver induced by a high fat diet in a rat experimental model: a histological and immunohistochemical study. *Int. J. Morphol., 41(6)*:1887-1896, 2023.

SUMMARY: The therapeutic effect of a granulocyte-colony stimulating factor (G-CSF) biosimilar drug, zarzio, on non-alcoholic fatty liver disease (NAFLD) in a rat model was investigated in this study. Thirty-two rats were randomly divided into four groups. Groups I and II were fed a standard laboratory diet, whereas groups III and IV were fed a high fat diet (HFD) for 14 weeks. After 12 weeks of feeding, groups I and III were administered normal saline, and groups II and IV were intraperitoneally administered zarzio (200 mg/kg/day) for two consecutive weeks. Hematoxylin-eosin (H&E) staining was used to assess hepatic and pancreatic morphology in all groups , oil red O (ORO) staining for lipid accumulation, Masson's staining for fibrosis, and immunohistochemistry assay for hepatic protein expression of insulin receptor substrate 1 (IRS1), nuclear factor erythroid 2-related factor 2 (Nrf2), tumour necrosis factor alpha (TNF-α) and pancreatic caspase-3. The NAFLD rats (group III) developed hepatic steatosis with increased lipid accumulation, perisinusoidal fibrosis, upregulated IRS1, TNF-α (all $P<0.05$) without a significant increase in Nrf2 protein expression compared with normal control. In comparison, model rats treated with zarzio (group IV) showed significant rejuvenation of the hepatic architecture, reduction of fat accumulation, and fibrosis. This was accompanied by the upregulation of Nrf2, downregulation of IRS1 and TNF-α protein expression (all $P<0.05$). No correlation was detected between NAFLD and non-alcoholic fatty pancreas disease (NAFPD). However, the pancreatic β-cells in group III showed increased caspase-3 expression, which was decreased ($P<0.05$) in group IV. In conclusion, zarzio ameliorates NAFLD by improving the antioxidant capacity of liver cells, reducing hepatic IRS1, TNF-α protein expression and pancreatic β-cells apoptosis, suggesting that zarzio could be used as a potential therapy for NAFLD.

KEY WORDS: Non-alcoholic fatty liver disease; Zarzio; Granulocyte colony stimulating factor; Nuclear factor erythroid 2-related factor 2; Tumour necrosis factor alpha; Insulin receptor substrates.

INTRODUCTION

Non-alcoholic fatty liver disease (NAFLD) is characterized by the accumulation of lipids in hepatocytes (hepatic steatosis) without excessive intake of alcohol (Spiers *et al*., 2022). With an estimated incidence of 25%, NAFLD is currently the most prominent chronic liver disease worldwide, and its incidence continues to rise (Younossi *et al*., 2018). NAFLD comprises a wide range of liver lesions, that range from simple hepatic steatosis to hepatic steatosis accompanied by chronic inflammation (non-alcoholic steatohepatitis, NASH), which can ultimately lead over time to hepatic fibrosis, cirrhosis, and even hepatocellular carcinoma (Calzadilla Bertot & Adams, 2016).

The development and progression of NAFLD is closely linked to obesity, insulin resistance (IR), and type-2 diabetes mellitus (T2DM) (Younossi, 2019). Moreover, genetic predispositions that influence hepatic fat metabolism, dietary fructose levels, and a lack of physical activity have also been shown to be contributory factors (Juanola *et al*., 2021). The pathogenesis of NAFLD was initially described by the two-hit hypothesis (Day & James, 1998), although a multiple-hit hypothesis has also been proposed (Polyzos *et al*., 2009). The first hit involves lipid accumulation in the form of triglycerides, and a concomitant increase in insulin resistance resulting in simple liver steatosis. This is followed

Department of Medical Emergency Services, College of Health Sciences-AlQunfudah,Umm Al-Qura University, Makkah, Saudi Arabia.

Received: 2023-08-23 Accepted: 202310-15

by multiple events, such as oxidative stress (OS), mitochondrial abnormalities, and the production of inflammatory cytokines, which contribute to NAFLD progression (Polyzos *et al*., 2009). However, precise mechanisms underlying the complex pathogenesis of NAFLD remain unclear.

OS plays a fundamental role in NAFLD development (Smirne *et al*., 2022). OS has been observed in experimental models of NAFLD (Ore & Akinloye, 2019) as well as in patients with NAFLD who demonstrated increased formation of reactive oxygen species (ROS) and decreased in the activity of antioxidant (Madan *et al*., 2006). Nuclear factor erythroid 2-related factor 2 (Nrf2), a cytoprotective transcription factor that plays a crucial role in cellular defence against OS by activating the transcription of antioxidant response elements (ARE) of antioxidant and cytoprotective genes. (Solano-Urrusquieta *et al*., 2020). A growing body of evidence indicates that the activation of the Nrf2/ARE signalling pathway, which is disrupted in NAFLD, can protect hepatocytes from oxidative stress and halt the progression of NAFLD (Solano-Urrusquieta *et al*., 2020; Zhou *et al*, 2022). As a result, the Nrf2/ARE signalling pathway has been identified as a potential therapeutic target approach for the treatment of NAFLD (Zhou *et al*, 2022).

The activation of proinflammatory cytokines, such as tumour necrosis factor alpha (TNF-α) in liver tissue has been also linked to the development and progression of NAFLD (Lu *et al*., 2022). An increased expression of TNF-α has been associated with the development of NAFLD in animal models (Ma *et al*., 2008; Wandrer *et al*., 2020) and in NASH patients where its expression seems to correlate with the severity of NASH (Paredes-Turrubiarte *et al*., 2016). Furthermore, blocking TNF-α signalling through TNF-receptor-1 was found to reduce liver steatosis, hepatocellular injury, and fibrosis in NAFLD animal models, suggesting a potential target of TNF-α signalling in NAFLD treatment (Wandrer *et al*., 2020).

Similar to NAFLD, non-alcoholic fatty pancreas disease (NAFPD), defined by pancreatic fat accumulation, has been associated with obesity, IR and T2DM (Shah *et al*., 2019). However, several studies have reported the association between NAFLD and NAFPD (van Geenen *et al*., 2010; Rugivarodom *et al*., 2022) but not in all (Heni *et al*., 2010; Koyuncu Sokmen *et al*., 2021) and the link remains controversial.

Granulocyte-colony stimulating factor (G-CSF) is a hematopoietic growth factor that modulates neutrophil development and formation from myeloid progenitors and promotes neutrophil mobilization from the bone marrow into the peripheral circulation (Hamilton & Achuthan, 2013). Several studies have shown that G-CSF has therapeutic effects against various liver diseases, including alcoholic steatohepatitis (Spahr *et al*., 2008), and non-alcoholic hepatic steatosis (Song *et al*., 2013; Song *et al*., 2015). The filgrastim drug, zarzio, a biosimilar non-glycosylated recombinant human G-CSF, is used to safeguard against against neutropenia in patients receiving cytotoxic chemotherapy for malignancy (Tharmarajah *et al*., 2014). In this study, the potential effect of zarzio on the amelioration of NAFLD induced by a high-fat diet (HFD) in rats was investigated. Possible mechanisms underlying this beneficial effect were also explored; specifically, zarzio's effects on the expression of the insulin resistance substrate 1 (IRS1) protein, TNF-α proinflammatory cytokine, and anti-oxidative stress protein, Nrf2. Furthermore, the correlation between NAFLD and NAFPD was evaluated.

MATERIAL AND METHOD

Experimental animals: Male albino rats weighing 150–180 g were used in the present study. They were confined in separate animal cages with *ad libitum* unrestricted access to food and water under standard experimental settings (12 h day/night cycle, 24±2 °C room temperature). Before commencing the experiment, the animals were acclimatized to their surroundings for one week. Animal handling and procedures were performed according to the guidelines of National Institutes of Health for the Care and Use of Laboratory Animals (NIH publications, No.85-23, 1996) and approved by Experimental Committee for Animal Research, Department of Pharmacology and Toxicology, Faculty of Medicine, Al-Azhar University.

Experimental design and treatments

Thirty-two rats were assigned randomly to four experimental groups (n=8) as described below:

Normal diet (ND) control group I: Rats were fed a standard laboratory rat diet for 14 weeks. After 12 weeks of feeding, all rats were administered 0.1 ml normal saline (Fisher Scientific, USA) intraperitoneally for 2 consecutive weeks.

ND+zarzio group II: Rats were fed a standard laboratory rat diet for 14 weeks. After 12 weeks of feeding, all rats were treated intraperitoneally with zarzio (Sandoz Egypt Pharma S.A.E., Novartis company) (200 mg/kg/day) (Joo *et al*., 2020) prepared in normal saline for 2 consecutive weeks.

HFD group III: Rats were fed a high fat diet (HFD) containing 87.7 % standard diet (w/w), 10 % pork fat (w/w), 2 % cholesterol (w/w) and 0.3 % bile salt (w/w) (Pan *et al*., 2006) for 14 weeks. After 12 weeks of feeding, all rats were administered 0.1ml normal saline intraperitoneally for 2 consecutive weeks.

HFD+zarzio group IV: Rats were fed an HFD for 14 weeks. After 12 weeks of feeding, all rats were intraperitoneally administered zarzio (200 mg/kg/day) for two consecutive weeks.

Rats were anaesthetized twenty-four hours after the last treatment with ether before being euthanized by cervical dislocation, and fresh liver and pancreatic tissues were collected from all experimental groups. Subsequently, tissue samples were fixed in 10 % neutral buffered formalin at 4°C for 24 h. Others were frozen in liquid nitrogen immediately and kept at -80°C to be used for other experiments.

Hematoxylin-eosin (H&E) staining. Sections of 4 μm in thickness were cut from liver and pancreatic tissue samples and stained with hematoxylin and eosin using standard procedure (Gamble, 2008).Stained sections were observed for histological alterations under a light microscope (Lecia DM500, Leica Biosystems).

Oil red O (ORO) staining. To detect lipid deposition in tissues, ORO staining was used as described by Song *et al*. (2015).Positively stained areas for ORO were analysed using Image-Pro Plus (version 6.0; Media Cybernetics, USA). Ten areas were randomly selected from individual sections and examined at 200x magnification. Lipid deposition was calculated as the ratio of the area of the ORO stained lipid droplets to the total tissue area (Song *et al*., 2015)

Masson's trichrome staining. Liver sections from different groups were stained using Masson's trichrome to detect liver fibrosis, as described previously (Jones, 2008). For quantifying of fibrosis, images of stained liver sections from each experimental treatment were obtained using a BX51 Olympus optical microscope equipped with an Olympus XC50 camera (Olympus Corporation, Japan). Image analysis was carried out using NIH ImageJ software (version 1.48v, MD, USA). Ten random selected fields in each section were analysed at 200x magnification and the collagen fractions (% area) were calculated by dividing the fibrotic areas within each field by the total field area and expressed as fractions of 100 % (Adebiyi *et al*., 2016).

Immunohistochemical assay. IRS1, caspase-3, TGF-α, and Nrf2 protein expressions were evaluated by immunohistochemistry using a horseradish peroxidase/diaminobenzidine(HRP/DAB) avidin biotin complex (ABC) detection immunohistochemical IHC Kit (Abcam, UK) as per the manufacturer's instructions. Antigen retrieval step was was carried out by dipping tissue sections in 10 mM citrate buffer (pH 6) and were incubated for 1 h in a 95°-100°C water. For inhibiting endogenous peroxidase activities, tissues were treated with a hydrogen peroxide block reagent (Abcam, UK) at room temperature for 10 min. To prevent non-specific binding, the kit protein block reagent was employed for 10 min at room temperature.Tissue sections were then incubated with primary antibody rabbit polyclonal anti-IRS1(1:500, #GB111506, servicebio, China), rabbit polyclonal anti-NRF2 (1:1000 #GB113808, servicebio, China), rabbit polyclonal anti-TNF-α (1:400, #GB11188, servicebio, China) and rabbit polyclonal anti-Caspase-3 (1:500, #GB11532, servicebio, China) overnight at 4 °C. The next day, sections were incubated with secondary antibody at room temperature for 1 h, followed by streptavidin-peroxidase enzyme conjugate for 10 min. Finally, sections were incubated for 1–10 min with 3,3-diaminobenzoic acid (DAB) substrateuntil a brown signal was observed, then counterstained withhematoxylin and checked under a light microscope. To quantify immunostaining, ten random fields from each section were examined and the percentage area staining for IRS1, Nrf2 and TNF-α was calculated using NIH ImageJ software.

Statistical analysis. Using SPSS software (version 17, IBM Corp, Armonk, NY, USA), analysis of variance (ANOVA) and Tukey's post-hoc multiple comparisons were conducted to determine the statistical significance of the experimental groups. All data are expressed as mean±standard error of mean (mean±SEM). The statistical significance level was deemed at P-value<0.05.

RESULTS

H&E and ORO staining. Using H&E and ORO-stained tissue sections, changes in the histological structure and lipid content of the rat liver and pancreas were analysed in all treatment groups.

ND control group I: Examination of H&E-stained liver sections from the normal diet group I (Fig. 1A) showed normal hepatic histology with neatly and tightly arranged anastomosing plates of hepatocytes separated by sinusoids emanating from the central vein. Hepatocytes were normal in size and morphology, with large round vesicular nuclei and uniform cytoplasm. Pancreatic sections revealed normal exocrine and endocrine pancreatic components (Fig. 2A). The exocrine portion is densely packed with pancreatic acini

of various shapes and sizes and lined with large pyramidal cells that have round, vesicular nuclei at their bases and prominent nucleoli (Fig. 2A). Acinar cells cytoplasm displayed apical acidophilia and basal basophilia, with some binucleated acinar cells. The endocrine portion, represented by the islets of Langerhans, was normal and appeared rounded, pale-stained area dispersed among darkly stained pancreatic acini (Fig. 2A). Each pancreatic islet is composed of a cord of cells separated by blood vessels. Most pancreatic beta cells were found in the central region of the islets, with rounded and lighter nuclei. Alpha cells with oval, darkly stained nuclei were located peripheral to the islets (Fig. 2A). ORO-stained liver and pancreatic sections from this group (Figs. 3A,E) showed very few lipid deposits.

Group II (ND+zarzio): Histological structure and lipid deposition in the liver (Figs. 1B and 3B) and pancreatic sections (Figs. 2B and 3F) obtained from this group were comparable to those of control group I.

Group III (HFD): Examination of H&E-stained liver sections from this group (Figs. 1C,D insert) revealed a large amount of vacuolar-like hepatic steatosis induced by NAFLD, with an almost complete absence of intrahepatic sinusoids. Hepatocytes appeared swollen and displayed varying degrees of cytoplasmic vacuolation; some contained multiple small fat vacuoles, some had a mixture of small and large fat vacuoles, and others appeared ballooned with single, large, fat vacuoles. H&E-stained pancreatic sections (Fig. 2C) showed some degree of cytoplasmic vacuolation of islet cells and a normal exocrine pancreas. ORO-stained liver sections (Fig. 3C) showed more prominent lipid accumulation in the liver, with a significant increase in the percentage of lipid deposits (P>0.05), compared to group I (Fig. 4). However, pancreatic sections (Fig. 3G) showed no apparent increase in lipid deposition.

Group IV (HFD+zarzio): H&E-stained liver sections (Fig. 1E) revealed improved hepatic architecture with the reappearance of intrahepatic sinusoids. Most hepatocytes were arranged neatly with less marked vacuolar-like steatosis and an absence of balloon degeneration compared with those in group III. Lipid deposition and droplet size in the liver were less prominent, as observed by ORO staining (Fig. 3D), and there was a significant reduction (*P*>0.05) in the percentage of lipid deposits compared to those of group III (Fig. 4). H&E (Fig. 2D) and ORO staining (Fig. 3H) of the pancreatic sections of this group were comparable to those of control group I.

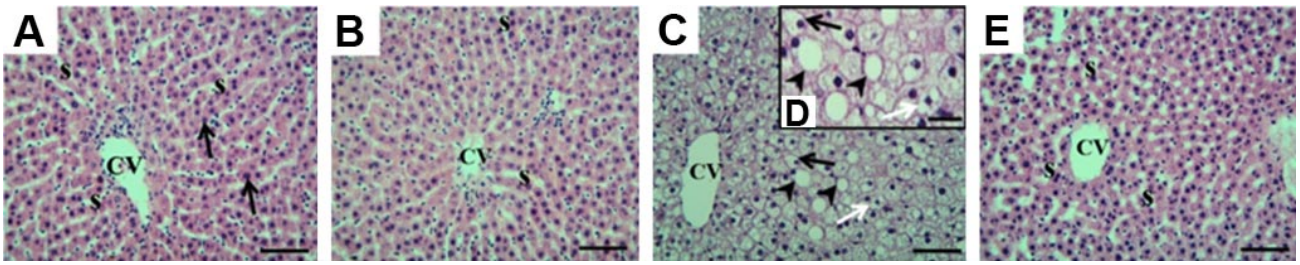

Fig. 1. Photomicrographs of hematoxylin-eosin-stained liver sections from each experimental group. (A) Normal diet (ND) group I shows normal hepatic arrangement with normal hepatocytes (black arrows), central vein (CV) and sinusoid (S). (B) Group II shows similar histological features as group I. (C, D insert) High-fat diet (HFD) group III shows vacuolar-like hepatic steatosis and an almost complete absence of intrahepatic sinusoids with some hepatocytes containing multiple small vacuoles (black arrows), some with a mixture of small and large vacuoles (white arrows), and others with large, single vacuoles (arrowheads). (E) Group IV treated with zarzio shows rejuvenated hepatic morphology with the reappearance of intrahepatic sinusoids (s), less marked vacuolar-like steatosis and absence of balloon degeneration in hepatocytes. (scale bar=50 μm; insert scale bar=25 μm).

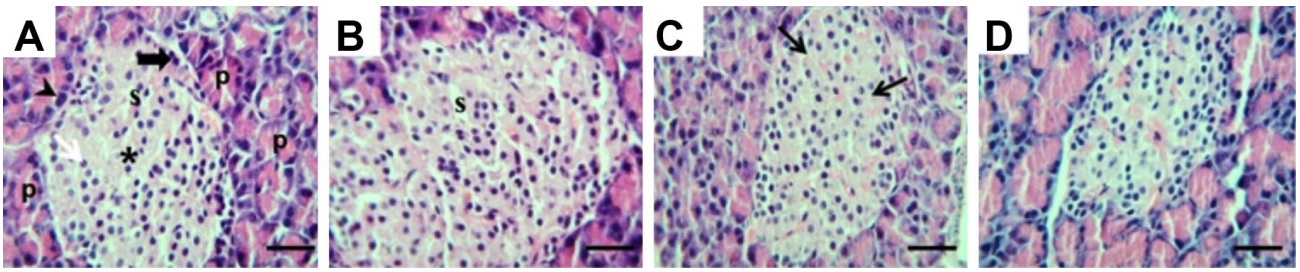

Fig. 2. Photomicrographs of hematoxylin-eosin-stained pancreatic sections from each experimental group. (A) Normal diet (ND) group I shows normal exocrine pancreas and endocrine pancreatic islets (*).(B) Group II shows similar histological features as group I. (C) The high-fat diet (HFD) group III shows some degree of cytoplasmic vacuolation (black arrows) of the islets and normal exocrine pancreas. (D) Group IV revealed normal histological pancreatic features comparable to those of the ND control group I. P, pancreatic acini; S, blood sinusoids; arrowhead, binucleated acinar cells; white arrow, islet beta-cells; thick black arrow, isl*et al*pha-cells. (scale bar=50 μm).

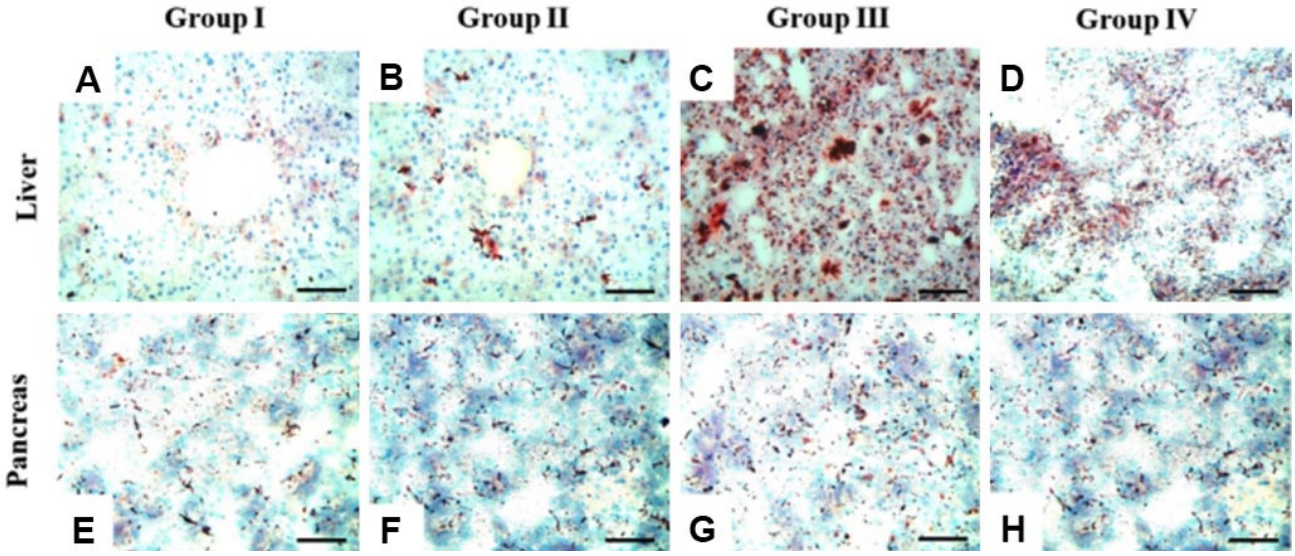

Fig. 3. Photomicrographs of oil red O staining in liver (A-D) and pancreatic (E-H) sections from each experimental group. Red vesicles indicate lipid deposits. (A) Normal diet (ND) group I represents normal liver control. (B) Group II shows a similar staining pattern as the control group I. (C) The high-fat diet (HFD) group III shows high lipid deposition. (D) Group IV HFD group treated with zarzio shows less lipid deposition compared to group III. (E-H) Pancreatic sections from each experimental group show no changes in lipid accumulation. (scale bar=50 μm).

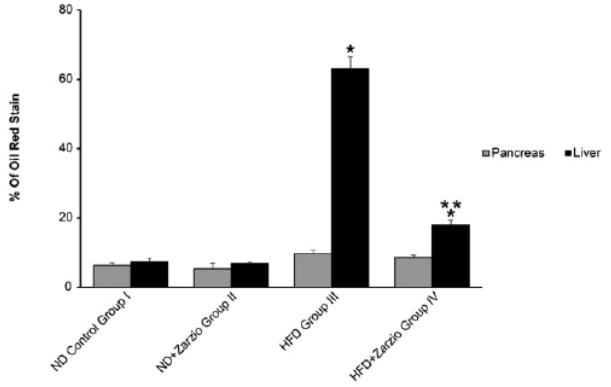

Fig. 4. Quantitative analysis of liver and pancreas sections stained with oil red O (ORO) in all experimental groups. The mean percentage of ORO-stained areas was calculated for ten randomly chosen fields of each section (n=4). Data represent mean±SE. * indicates significance versus normal diet (ND) control group I; ** indicates significance versus high-fat diet (HFD) group III when P<0.05

Masson's trichrome staining. Masson's trichrome stained liver sections from control group I, displayed a normaldistribution ofblue-stained collagen fibres around the central veins (Fig. 5A). Group II rats fed a normal diet and treated with zarzio showed Masson's trichrome staining comparable to that of group I rats (Fig. 5B). However, the HFD group III had pericellular and perisinusoidal fibrosis, most pronounced in zone 3 near the central vein, with thick collagen fibres extending from the vicinity of the central vein invading spaces between the hepatocytes (Figs. 5C,D, insert). HFD group IV treated with zarzio showed significantly less pericellular and perisinusoidal fibrosis than the untreated group III (Fig. 5E). Percentage analysis of fibrosis in each group (Fig. 6) showed a pronounced increase (P<0.05) in HFD group III compared to that in normal group I. This increase in fibrosis was significantly reduced in HFD group IV treated with zarzio.

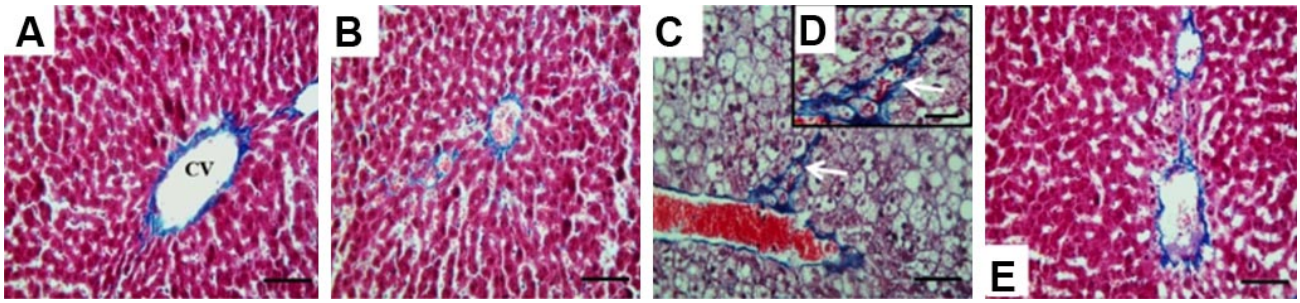

Fig. 5. Photomicrographs of Masson's trichrome staining in liver sections from each experimental group. (A) Normal diet (ND) group I shows normal fine collagen distribution. (B) Group II shows similar staining pattern as control group I. (C and D insert) High-fat diet (HFD) group III shows extension of blue-stained collagen fibres from the vicinity of the central vein invading spaces between the hepatocytes (white arrows), indicative of pericellular and perisinusoidal fibrosis. (E) HFD Group IV treated with zarzio shows collagen fibres distribution similar to the control group. (scale bar=50 μm; insert scale bar=25 μm).

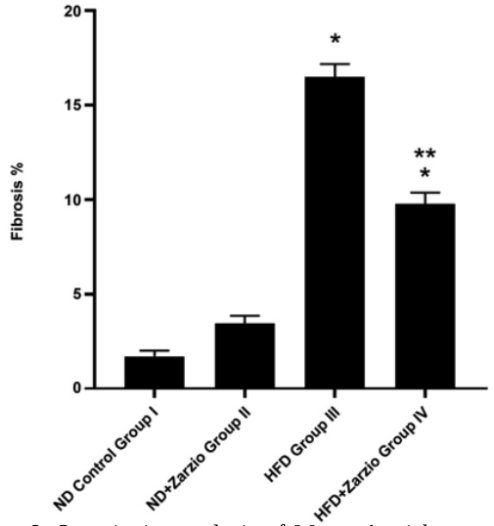

Fig. 6. Quantitative analysis of Masson's trichrome-stained liver sections in all experimental groups. The mean percentage of fibrotic areas was calculated for ten randomly chosen fields of each section (n=4). Data represent mean±SE. * indicates significance versus normal diet (ND) control group I; ** indicates significance versus high-fat diet (HFD) group II when P<0.05.

Immunohistochemical assay. To evaluate the treatment effect of zarzio on the protein expression of hepatic IRS1, TNF-α, Nrf2 and pancreatic caspase-3 in the NAFLD rat model, IHC assays were carried out in all experimental groups (Fig. 7). Rat livers of ND groups I and II showed low numbers of IRS1 (Figs. 7A,B), TNF-α (Figs. 7E,F), and Nrf2-positively (Figs. 7I,J) stained cells. As compared to ND control group I, HD group III displayed a higher number of IRS1 (Fig. 7C), TNF-a (Fig. 7G) and a moderate number of Nrf2-positively (Fig. 7K) stained cells. However, HD group IV treated with zarzio had a moderate number of IRS1 (Fig. 7D), TNF-α (Fig. 7H) and a higher number of Nrf2-positively (Fig. 7L) stained cells compared to group III. A high number of pancreatic caspase-3-positively stained cells was detected in HD group III (Fig. 8C) compared to group I (Fig. 8A) and was restricted to pancreatic islet beta cells (Fig. 8C). Group IV (Fig. 8D) showed few pancreatic caspse-3-positively stained cells compared to group III. Quantification of the immunostaining expression revealed a significant increase (P<0.05) in IRS1 (Fig. 7M) and TNF-α (Fig. 7N) and

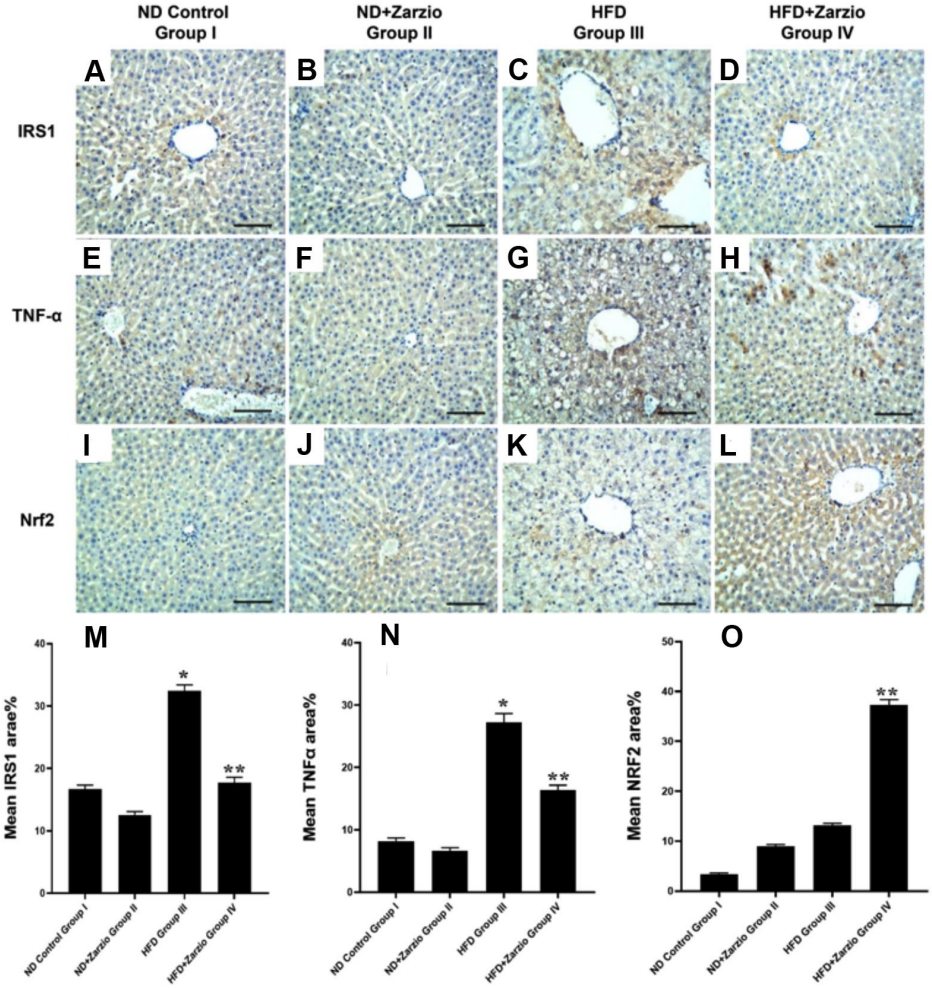

Fig. 7. Photomicrographs of immunohistochemically-stained liver sections for IRS1,TNF-a and Nrf2 protein expression in all experimental groups showing weak expression in the normal diet (ND) groups I (7A,7E and 7I) and II (7B,7F AND 7J), strong expression for IRS1(7C), TNF-α (7G)and weak expression for Nrf2 (7K)in the high-fat diet (HFD) group III and moderate to weak expression for IRS1 (7D), TNF-α (7H)and strong expression for Nrf2 (7L) in HFD group IV treated with zarzio. 7M, 7N and 7O represent quantitative analysis of immunohistochemically - stained liver sections for IRS1, TNF-α and Nrf2 in all experimental groups. The mean percentage of stained area was calculated for ten randomly chosen fields of each section (n=4). Data represent mean±SE. * indicates significance versus ND control group I; ** indicates significance versus HFD group II when *P*<0.05. (scale bar=50 μm).

decreased (P<0.05) Nrf2 (Fig. 7O) expression in HD group III compared to control group I. The increase in IRS1, TNF-α and decrease in Nrf2 expression observed in group III was significantly reversed in group IV compared with that in group III. Pancreatic caspase-3 expression was significantly increased (*P*<0.05) in pancreatic islet beta cells in group III compared to that in the control group I (Fig. 8E). However, group IV demonstrated a significant reduction (*P*<0.05) in pancreatic caspase-3 expression compared to group III (Fig. 8E).

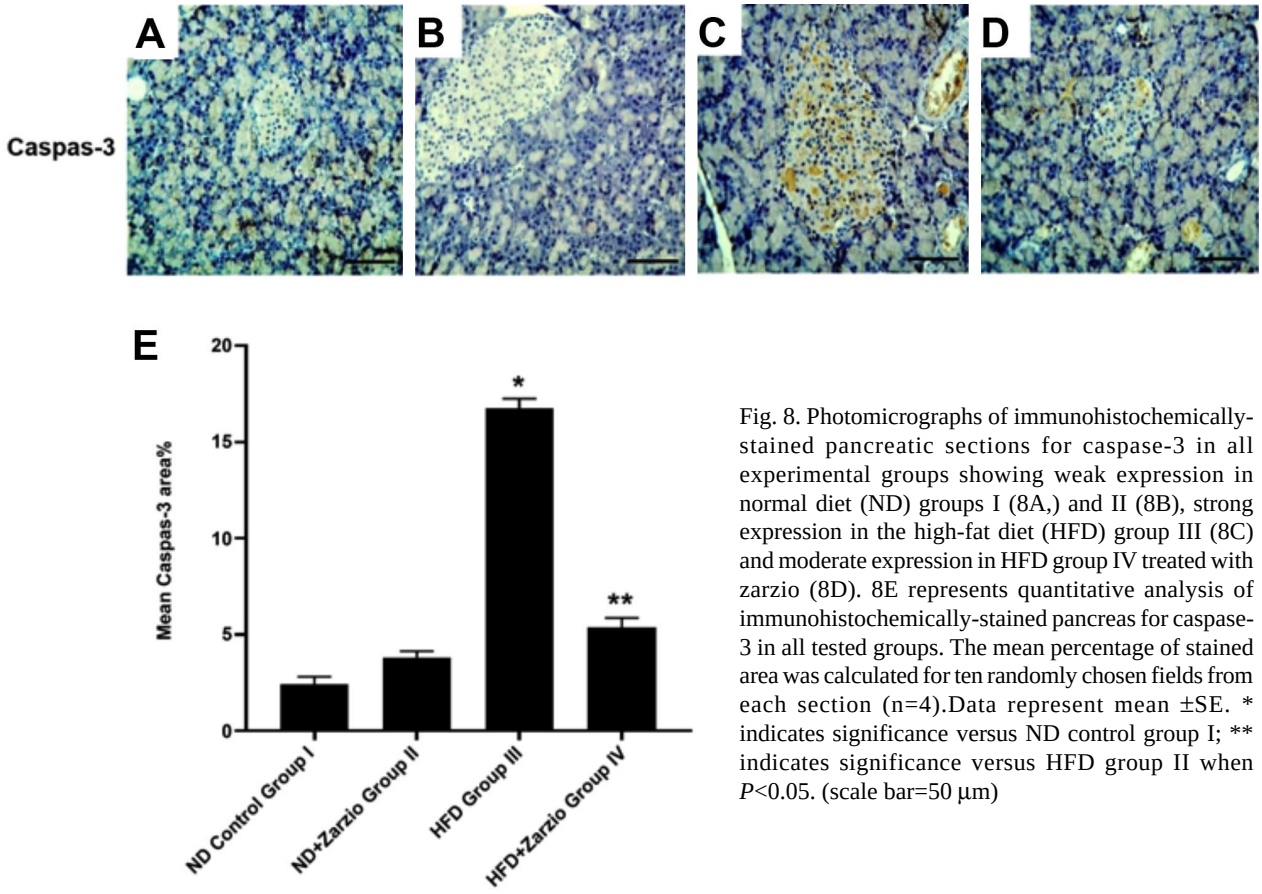

Fig. 8. Photomicrographs of immunohistochemically-stained pancreatic sections for caspase-3 in all experimental groups showing weak expression in normal diet (ND) groups I (8A,) and II (8B), strong expression in the high-fat diet (HFD) group III (8C) and moderate expression in HFD group IV treated with zarzio (8D). 8E represents quantitative analysis of immunohistochemically-stained pancreas for caspase-3 in all tested groups. The mean percentage of stained area was calculated for ten randomly chosen fields from each section (n=4).Data represent mean ±SE. * indicates significance versus ND control group I; ** indicates significance versus HFD group II when *P*<0.05. (scale bar=50 μm)

DISCUSSION

Globally, the prevalence of NAFLD is increasing, and it has become the leading cause of chronic liver disease, consistent with the rising incidence of obesity (Younossi *et al*., 2018). Currently, there are no proven therapies for NAFLD, and modifying risk factors, particularly those associated with lifestyle, is the only available option. Therefore, there is a need for more effective drug treatments. The results of this study are discussed from three perspectives. First, a rat model of NAFLD was developed by feeding rats a high-fat diet; second, the effects and underlying mechanisms of zarzio treatment against changes induced by a high-fat diet were studied; and third, the correlation between NAFLD and NAFPD was investigated. In this study, an experimental model of rats with NAFLD was developed by providing rats with a high-fat diet for 14 weeks. The validity and successful establishment of the NAFLD model were confirmed by histological findings of hepatic steatosis, as demonstrated by ballooning hepatocytes with varying degrees of cytoplasmic vacuolation, the absence of intrahepatic sinusoids, and excessive lipid droplet accumulation compared to rats on a regular diet, consistent with previous reports (Song *et al*., 2013, 2015; Deng *et al*., 2019).

Previous studies in rats have found that G-CSF treatment ameliorates non-alcoholic hepatic steatosis (Song *et al*., 2013) and prevents the formation of hepatic steatosis (Song *et al*., 2015). The current study revealed, that zarzio ameliorated HFD-induced hepatic steatosis, confirming the therapeutic effect of G-CSF. Histologically, treatment with zarzio significantly reduced the ballooning of hepatocytes and lipid droplet accumulation observed in the liver tissues of the model group and caused an overall rejuvenation of hepatic architecture. To clarify the mechanism underlying the beneficial effects of zarzio, its effect on the expression

of IRS-1, TNF-α, and Nrf2 proteins was evaluated. NAFLD is usually accompanied by dysregulation of insulin signalling pathways, IRS-1 and IRS-2, resulting inIR (Sakurai *et al*., 2021). In the liver, IR stimulates the upregulation of lipogenic proteins, for example sterol regulatory element-binding protein-1c (SREBP-1c), which regulates positively the level of expression of genes involved in de novo lipid synthesis (Xu *et al*., 2013). In NAFLD, SREBP-1c was shown to be significantly expressed (Kohjima *et al*., 2008; Song *et al*., 2015) and is correlated with an increase in IRS-1 expression (Kohjima *et al*., 2008). In the present study, the NAFLD model group showed a significant increase in IRS-1 expression, consistent with Kohjima *et al*. (2008). The present study also demonstrated that treatment with zarzio significantly reduced IRS-1 expression in the model group. Several reports have shown that the therapeutic effects of G-CSF in ameliorating non-alcoholic hepatic steatosis involve a reduction in SREBP-1c expression (Song *et al*., 2013, 2015). Therefore, it can be postulated that the reduction in IRS-1 expression by zarzio may suppress de *novo* lipid synthesis by down-regulating SREBP-1c protein expression.

OS plays an important role in the development of NAFLD (Smirne *et al*., 2022) and the activation of the signalling pathway involving Nrf2, which is disrupted in NAFLD. Nrf2 is a positive regulator of genes that protect against OS and a negative regulator of genes that contribute to hepatosteatosis by suppressing lipogenesis and promoting fatty acid oxidation (Chambel *et al*., 2015). Nrf2 has also been shown to protect hepatocytes from OS and halt the progression of NAFLD (Zhou *et al*., 2022). The findings of the present study indicate that Nrf2 protein expression was slightly, but not significantly elevated in the livers of rats with HFD-induced NAFLD, indicating that there is insufficient activation of the Nrf2 signalling pathway to protect against OS and prevent the development and progression of NAFLD (Zhou *et al*., 2022). Furthermore, the present study revealed that treatment of the NAFLD model group with zarzio significantly increase Nrf2 expression, indicating that signalling pathway involving Nrf2 may be a key target of zarzio in the treatment and prevention of NAFLD.

An HFD and associated OS could activate intracellular inflammatory pathways in hepatocytes by promoting inflammatory cytokine synthesis, such as TNF-α (Lu *et al*., 2022). TNF-a acts by activating the transcription factor, NF-kB, causing an increase in the transcription of inflammation-associated proteins such as TNF-α and interleukin (IL)-6, which in turn enhances TNF-α signalling causing further liver damage (Zhang *et al*., 2017). Consequently, elevated TNF-α plays a central role in the development of NAFLD, particularly in the transition of simple hepatic steatosis to NASH (Lu *et al*., 2022). Additionally, TNF-α plays pivotal role in the development of IR by suppressing the tyrosine kinase activity of the insulin receptor and promoting the serine phosphorylation of IRS-1 (Asrih & Jornayvaz, 2013). In this study, the NAFLD group showed high levels of TNF-α protein expression, in line with a prior study (Lu *et al*., 2022). In contrast, the NAFLD group treated with zarzio showed a significant reduction in TNF-α expression, indicating a potential anti-inflammatory effect of the drug. This anti-inflammatory action exerted by zarzio may be due to Nrf2 activation, which prevents inflammation via inhibition of the NF-kB pathway (Song *et al*., 2018).

Fibrosis, a result of enhanced collagen deposition, is tightly linked to chronic hepatic inflammation and is a key feature that controls the progression of NAFLD to cirrhosis (Perumpail *et al*., 2017). Typically, hepatic fibrosis begins in the perisinusoidal regions and advances to include the portal areas, followed by the formation of fibrotic bridges between the central vein and portal tract, culminating in cirrhosis (Albhaisi & Sanyal, 2019). In the present study, histopathological assessment (Masson staining) was conducted to detect liver fibrosis in the model group, revealing very mild perisinusoidal fibrosis, most noticeable in zone 3 near the central vein, indicating early stages of fibrosis and possibly early stages of disease progression in the model group (Xu *et al*., 2010). This increase in collagen deposition may be due to an increase in hepatic stellate cells (HSC) activity, which is the main driver of hepatic fibrosis in damaged livers (Kisseleva & Brenner, 2021). In contrast, the NAFLD group treated with zarzio showed a decline in fibrosis, suggesting that zarzio may hinder the progression of fibrosis in NAFLD.

As pancreatic and liver tissues are derived from the same embryonic endoderm (Ghurburrun *et al*., 2018) and seeing that both NAFLD and NAFPD are linked to obesity, IR, and T2DM (Shah *et al*., 2019), researchers have postulated that both diseases could have similar aetiologies. However, the association between NAFLD and NAFPD is controversial. In the current study, no histological changes or significant lipid accumulation were observed in the pancreas of the model group. However, cytoplasmic vacuolation of the islet cells was detected. The lack of correlation observed between fat accumulation in the liver and pancreas in this study may be due to the different molecular mechanisms that mediate the pathophysiology of NAFLD and NAFPD, as reported by Shah *et al*. (2019). Furthermore, fatty pancreas has been reported to be significantly associated with more severe histologic features of NAFLD and a higher fibrotic stage, which was not observed in the NAFLD model in this study (Rosenblatt *et al*., 2019).

NAFLD and T2DM often occur together and are closely associated with obesity and IR (Ming-Feng *et al*., 2019). One of the characteristic features of T2DM is β-cells dysfunction in the pancreas, which is caused by an increased workload and glucolipotoxicity (Schultheis *et al*., 2019). In the current study, β-cells in the NAFLD group revealed an increased apoptotic incidence. Conversely, the NAFLD model treated with zarzio presented a decline in β-cells apoptosis. The current results suggest that zarzio may protect β-cells from apoptosis possibly by activating Nrf2, supressing OS as a major mediator of β-cell glucolipotoxicity and promoting b-cell proliferation (Schultheis *et al*., 2019; Baumel-Alterzon *et al*., 2022).

In conclusion, the current study demonstrates that zarzio ameliorates NAFLD induced by HFD in a rat model. The potential mechanism of action of this effect involves reducing lipid accumulation, fibrosis, and expression of IRS-1 and increasing Nrf2 expression and preventing islet-cell apoptosis. However, further in studies are required to fully elucidate zarzio's precise mechanism of action and clinical effect. A limitation of this study is that the response to treatment may vary according to disease progression and the stage of fibrosis; thus, the impact of zarzio must be assessed in NAFLD models with severe fibrosis.

ACKNOWLEDGMENTS

The author is grateful to the university for providing the resources and databases used in this research. I would like to thank Professor Ali Ahmed Abosaif, Department of Pharmacology and Toxicology, Faculty of Medicine, Al-Azhar University and Dr Ahmed Alsherbini, Department of Pharmacy, Heliopolis University for their help with the animal work.

BAOKBAH, T. A. S. Zarzio mejora el hígado graso no alcohólico inducido por una dieta rica en grasas en un modelo experimental en ratas: un estudio histológico e inmunohistoquímico. *Int. J. Morphol., 41(6)*:1887-1896, 2023.

RESUMEN: En este estudio se investigó el efecto terapéutico de un fármaco biosimilar del factor estimulante de colonias de granulocitos (G-CSF), zarzio, sobre la enfermedaddel hígado graso no alcohólico (NAFLD) en un modelo de rata. Treinta y dos ratas se dividieron aleatoriamente en cuatro grupos. Los grupos I y II fueron alimentados con una dieta estándar de laboratorio, mientras que los grupos III y IV fueron alimentados con una dieta alta en grasas (HFD) durante 14 semanas. Después de 12 semanas de alimentación, a los grupos I y III se les administró solución salina normal, y a los grupos II y IV se les administró zarzio por vía intraperitoneal (200 mg/kg/día) durante dos semanas consecutivas. Se utilizó tinción de hematoxilina-eosina (H&E) para evaluar la morfología hepática y pancreática en todos los grupos, tinción con rojo aceite O (ORO) para la acumulación de lípidos, tinción de Masson para la fibrosis y ensayo de inmunohistoquímica para la expresión de la proteína hepática del sustrato 1 del receptor de insulina (IRS1), factor nuclear eritroide 2 relacionado con el factor 2 (Nrf2), factor de necrosis tumoral alfa (TNF-α) y caspasa-3 pancreática. Las ratas NAFLD (grupo III) desarrollaron esteatosis hepática con aumento de la acumulación de lípidos, fibrosis perisinusoidal, IRS1 y TNF-α regulados positivamente (todos P <0,05) sin un aumento significativo en la expresión de la proteína Nrf2 en comparación con el control normal. En comparación, las ratas modelo tratadas con zarzio (grupo IV) mostraron un rejuvenecimiento significativo de la arquitectura hepática, una reducción de la acumulación de grasa y fibrosis. Esto estuvo acompañado por la regulación positiva de Nrf2, la regulación negativa de la expresión de la proteína IRS1 y TNF-α (todas P <0,05). No se detectó correlación entre NAFLD y la enfermedad del páncreas graso no alcohólico (NAFPD). Sin embargo, las células β pancreáticas en el grupo III mostraron una mayor expresión de caspasa-3, que disminuyó (P <0,05) en el grupo IV. En conclusión, zarzio mejora la NAFLD al mejorar la capacidad antioxidante de las células hepáticas, reduciendo el IRS1 hepático, la expresión de la proteína TNF-α y la apoptosis de las células β pancreáticas, lo que sugiere que zarzio podría usarse como una terapia potencial para la NAFLD.

PALABRAS CLAVE: Enfermedad del hígado graso no alcoholic; Zarzio; Factor estimulante de colonias de granulocitos; Factor 2 relacionado con el eritroide nuclear 2; Factor de necrosis tumoral alfa; Sustratos del receptor de insulina.

REFERENCES

Adebiyi, O. A.; Adebiyi, O. O. & Owira, P. M. Naringin reduces hyperglycemia-induced cardiac fibrosis by relieving oxidative stress. *PLoS One, 11(3)*:e0149890, 2016.

Albhaisi, S. & Sanyal, A. J. Applying Non-Invasive Fibrosis Measurements in NAFLD/NASH: Progress to Date. *Pharmaceut. Med., 33(6)*:451-63, 2019.

Asrih, M. & Jornayvaz, F. R. Inflammation as a potential link between nonalcoholic fatty liver disease and insulin resistance. *J. Endocrinol., 218(3)*:R25-R36, 2013.

Baumel-Alterzon, S.; Katz, L. S.; Brill, G.; Jean-Pierre, C.; Li, Y.; Tse, I.; Biswal, S.; Garcia-Ocaña, A. & Scott, D. K. Nrf2 regulates b-Cell mass by suppressing b-Cell death and promoting β-Cell proliferation. *Diabetes, 71(5)*:989-1011, 2022.

Calzadilla Bertot, L. & Adams, L. A. The natural course of non-alcoholic fatty liver disease. *Int. J. Mol. Sci., 17(5)*:774, 2016.

Chambel, S. S.; Santos-Gonçalves, A. & Duarte, T. L. The dual role of Nrf2 in nonalcoholic fatty liver disease: regulation of antioxidant defenses and hepatic lipid metabolism. *Biomed Res. Int., 2015*:597134, 2015.

Day, C. P. & James, O. F. Steatohepatitis: a tale of two "hits"? *Gastroenterology, 114(4)*:842-5, 1998.

Deng, Y.; Tang, K.; Chen, R.; Nie, H.; Liang, S.; Zhang, J.; Zhang, Y. & Yang, Q. Berberine attenuates hepatic oxidative stress in rats with non-alcoholic fatty liver disease via the Nrf2/ARE signalling pathway. *Exp. Ther. Med., 17(3)*:2091-8, 2019.

Gamble, M. *The Hematoxylin and Eosin.* In: Bancroft, J. & Gamble, M. (Eds.). Theory and Practice of Histological Techniques. 6th ed. London, Churchill Livingstone, 2008. pp.121-34.

Ghurburrun, E.; Borbath, I.; Lemaigre, F. P. & Jacquemin, P. Liver and pancreas: do similar embryonic development and tissue organization lead to similar mechanisms of tumorigenesis? *Gene Expr., 18(3)*:149-55, 2018.

Hamilton, J. A. & Achuthan, A. Colony stimulating factors and myeloid cell biology in health and disease. *Trends Immunol., 34(2)*:81-9, 2013.

Heni, M.; Machann, J.; Staiger, H.; Schwenzer, N. F.; Peter, A.; Schick, F.; Claussen, C. D.; Stefan, N.; Häring, H. U. & Fritsche, A. Pancreatic fat is negatively associated with insulin secretion in individuals with impaired fasting glucose and/or impaired glucose tolerance: a nuclear magnetic resonance study. *Diabetes Metab. Res. Rev., 26(3)*:200-5, 2010.

Jones, M. *Connective Tissues and Stains*. In: Bancroft, J. & Gamble, M. (Eds.). Theory and Practice of Histological Techniques. 6th ed. London, Churchill Livingstone, 2008. pp.135-60.

Joo, H. W.; Song, Y. S.; Park, I. H.; Shen, G. Y.; Seong, J. H.; Shin, N. K.; Lee, A. H.; Kim, H. & Kim, K. S. Granulocyte colony stimulating factor ameliorates hepatic steatosis associated with improvement of autophagy in diabetic rats. *Can. J. Gastroenterol. Hepatol., 2020*:2156829, 2020.

Juanola, O.; Martínez-López, S.; Francés, R. & Gómez-Hurtado, I. Non-alcoholic fatty liver disease: metabolic, genetic, epigenetic and environmental risk factors. *Int. J. Environ. Res. Public Health, 18(10)*:5227, 2021.

Kisseleva, T. & Brenner, D. Molecular and cellular mechanisms of liver fibrosis and its regression. *Nat. Rev. Gastroenterol .Hepatol., 18(3)*:151-66, 2021.

Kohjima, M.; Higuchi, N.; Kato, M.; Kotoh, K.; Yoshimoto, T.; Fujino, T.; Yada, M.; Yada, R.; Harada, N.; Enjoji, M.; *et al*. SREBP-1c, regulated by the insulin and AMPK signaling pathways, plays a role in nonalcoholic fatty liver disease. *Int. J. Mol. Med., 21(4)*:507-11, 2008.

Koyuncu Sokmen, B.; Sahin, T.; Oral, A.; Kocak, E. & Inan, N. The comparison of pancreatic and hepatic steatosis in healthy liver donor candidates. *Sci. Rep., 11(1)*:4507, 2021.

Lu, S.; Wang, Y. & Liu, J. Tumor necrosis factor-a signaling in nonalcoholic steatohepatitis and targeted therapies. *J. Genet. Genomics, 49(4)*:269-78, 2022.

Ma, X.; Hua, J. & Li, Z. Probiotics improve high fat diet-induced hepatic steatosis and insulin resistance by increasing hepatic NKT cells. *J. Hepatol., 49(5)*:821-30, 2008.

Madan, K.; Bhardwaj, P.; Thareja, S.; Gupta, S. D. & Saraya, A. Oxidant stress and antioxidant status among patients with nonalcoholic fatty liver disease (NAFLD). *J. Clin. Gastroenterol., 40(10)*:930-5, 2006.

Ming-Feng, X.; Hua, B. & Xin, G. NAFLD and diabetes: two sides of the same coin? Rationale for gene-based personalized NAFLD treatment. *Front. Pharmacol., 10*:877, 2019.

Ore, A. & Akinloye, O. A. Oxidative stress and antioxidant biomarkers in clinical and experimental models of non-alcoholic fatty liver disease. *Medicina (Kaunas), 55(2)*:26, 2019.

Pan, M.; Song, Y. L.; Xu, J. M. & Gan, H. Z. Melatonin ameliorates nonalcoholic fatty liver induced by high-fat diet in rats. *J. Pineal Res., 41(1)*:79-84, 2006.

Paredes-Turrubiarte, G.; González-Chávez, A.; Pérez-Tamayo, R.; Salazar-Vázquez, B. Y.; Hernández, V. S.; Garibay-Nieto, N.; Fragoso, J. M. & Escobedo, G. Severity of non-alcoholic fatty liver disease is associated with high systemic levels of tumor necrosis factor alpha and low serum interleukin 10 in morbidly obese patients. *Clin. Exp. Med., 16(2)*:193-202, 2016.

Perumpail, B. J.; Khan, M. A.; Yoo, E. R.; Cholankeril, G.; Kim, D. & Ahmed, A. Clinical epidemiology and disease burden of nonalcoholic fatty liver disease. *World J. Gastroenterol., 23(47)*:8263-76, 2017.

Polyzos, S. A.; Kountouras, J. & Zavos, C. The multi-hit process and the antagonistic roles of tumor necrosis factor-alpha and adiponectin in non alcoholic fatty liver disease. *Hippokratia, 13(2)*:127-8, 2009.

Rosenblatt, R.; Mehta, A.; Snell, D.; Hissong, E.; Kierans, A. S. & Kumar, S. Ultrasonographic nonalcoholic fatty pancreas is associated with advanced fibrosis in NAFLD: a retrospective analysis. *Dig. Dis. Sci., 64(1)*:262-8, 2019.

Rugivarodom, M.; Geeratragool, T.; Pausawasdi, N. & Charatcharoenwitthaya, P. Fatty pancreas: linking pancreas pathophysiology to nonalcoholic fatty liver disease. *J. Clin. Transl. Hepatol., 10(6)*:1229-39, 2022.

Sakurai, Y.; Kubota, N.; Yamauchi, T. & Kadowaki, T. Role of insulin resistance in MAFLD. *Int. J. Mol. Sci., 22(8)*:4156, 2021.

Schultheis, J.; Beckmann, D.; Mulac, D.; Müller, L.; Esselen, M. & Düfer, M. Nrf2 activation protects mouse beta cells from glucolipotoxicity by restoring mitochondrial function and physiological redox balance. *Oxid. Med. Cell. Longev., 2019*:7518510, 2019.

Shah, N.; Rocha, J. P.; Bhutiani, N. & Endashaw, O. Nonalcoholic fatty pancreas disease. *Nutr. Clin. Pract., 34 Suppl. 1*:S49-S56, 2019.

Smirne, C.; Croce, E.; Di Benedetto, D.; Cantaluppi, V.; Comi, C.; Sainaghi, P. P.; Minisini, R.; Grossini, E. & Pirisi, M. Oxidative stress in non-alcoholic fatty liver disease. *Livers, 2(1)*:30-76, 2022.

Solano-Urrusquieta, A.; Morales-González, J. A.; Castro-Narro, G. E.; Cerda-Reyes, E.; Flores-Rangel, P. D. & Fierros-Oceguera, R. NRF-2 and nonalcoholic fatty liver disease. *Ann. Hepatol., 19(5)*:458-65, 2020.

Song, J.; Zhang, W.; Wang, J.; Yang, H.; Zhao, X.; Zhou, Q.; Wang, H.; Li, L. & Du, G. Activation of Nrf2 signaling by salvianolic acid C attenuates NF-kB mediated inflammatory response both in vivo and *in vitro*. *Int. Immunopharmacol., 63*:299-310, 2018.

Song, Y. S.; Fang, C. H.; So, B. I.; Park, J. Y.; Jun, D. W. & Kim, K. S. Therapeutic effects of granulocyte-colony stimulating factor on non-alcoholic hepatic steatosis in the rat. *Ann. Hepatol., 12(1)*:115-22, 2013.

Song, Y. S.; Joo, H. W.; Park, I. H.; Shen, G. Y.; Lee, Y.; Shin, J. H.; Kim, H. & Kim, K. S. Granulocyte-colony stimulating factor prevents the development of hepatic steatosis in rats. *Ann. Hepatol., 14(2)*:243-50, 2015.

Spahr, L.; Lambert, J. F.; Rubbia-Brandt, L.; Chalandon, Y.; Frossard, J. L.; Giostra, E. & Hadengue, A. Granulocyte-colony stimulating factor induces proliferation of hepatic progenitors in alcoholic steatohepatitis: a randomized trial. *Hepatology, 48(1)*:221-9, 2008.

Spiers, J.; Brindley, J. H.; Li, W. & Alazawi, W. What's new in non-alcoholic fatty liver disease? *Frontline Gastroenterol., 13(e1)*:e102-e108, 2022.

Tharmarajah, S.; Mohammed, A.; Bagalagel, A.; MacDonald, K. & Abraham, I. Clinical efficacy and safety of Zarzio® (EP2006), a biosimilar recombinant human granulocyte colony-stimulating factor. *Biosimilars, 4*:1-9, 2014.

van Geenen, E. J.; Smits, M. M.; Schreuder, T. C.; van der Peet, D. L.; Bloemena, E. & Mulder, C. J. Nonalcoholic fatty liver disease is related to nonalcoholic fatty pancreas disease. *Pancreas, 39(8)*:1185-90, 2010.

Wandrer, F.; Liebig, S.; Marhenke, S.; Vogel, A.; John, K.; Manns, M. P.; Teufel, A.; Itzel, T.; Longerich, T.; Maier, O.; *et al*. TNF-Receptor-1 inhibition reduces liver steatosis, hepatocellular injury and fibrosis in NAFLD mice. *Cell Death Dis., 11(3)*:212, 2020.

Xu, X.; So, J. S.; Park, J. G. & Lee, A. H. Transcriptional control of hepatic lipid metabolism by SREBP and ChREBP. *Semin. Liver Dis., 33(4)*:301-11, 2013.

Xu, Z. J.; Fan, J. G.; Ding, X. D.; Qiao, L. & Wang, G. L. Characterization of high-fat, diet-induced, non-alcoholic steatohepatitis with fibrosis in rats. *Dig. Dis. Sci., 55(4)*:931-40, 2010.

Younossi, Z. M. Non-alcoholic fatty liver disease - A global public health perspective. *J. Hepatol., 70(3)*:531-44, 2019.

Younossi, Z.; Anstee, Q. M.; Marietti, M.; Hardy, T.; Henry, L.; Eslam, M.; George, J.; & Bugianesi, E. Global burden of NAFLD and NASH: trends, predictions, risk factors and prevention. *Nat. Rev. Gastroenterol. Hepatol., 15(1)*:11-20, 2018.

Zhang, Q.; Lenardo, M. J. & Baltimore, D. 30 years of NF-kB: a blossoming of relevance to human pathobiology. *Cell, 168(1-2)*:37-57, 2017.

Zhou, J.; Zheng, Q. & Chen, Z. The Nrf2 pathway in liver diseases. *Front. Cell Dev. Biol., 10*:826204, 2022.

Corresponding author:
Dr. Tourki A. S. Baokbah
Department of Medical Emergency Services
College of Health Sciences-AlQunfudah
Umm Al-Qura university
SAUDI ARABIA

E-mail: tabaokbah@uqu.edu.sa

https://orcid.org/0000-0001-6091-198X